ELSEVIER

Surface Science 401 (1998) 269–281

surface science

Generation of "stabilized" surface species by low-energy interactions of ethylene ions with O- or N-precovered Cu(100) at room temperature

H. Yu, K.T. Leung *

Department of Physics and Department of Chemistry, The University of Waterloo, Waterloo, Ontario N2L 3G1, Canada

Received 15 August 1997; accepted for publication 8 December 1997

Abstract

The dissociative adsorption and surface reactions induced by low-energy ($\leq$200 eV) irradiation of unmass-selected ethylene ions on clean, O-precovered and N-precovered Cu(100) surfaces at room temperature (RT) were investigated by high-resolution electron energy loss spectroscopy (EELS) and temperature-programmed desorption mass spectrometry. Ion irradiation of a clean Cu(100) surface in ethylene at 200 eV impact energy was found to produce hydrocarbon fragments that adsorbed readily on the surface at RT and decomposed completely after annealing to above 600 K. For an O-precovered Cu(100) surface at RT, the hydrocarbon species so produced appeared to react with the pre-deposited O atoms to form "stabilized" CO. In addition to the red-shifted CO stretch observed at a low ethylene ion dose, a blue-shifted CO stretch was also found at a higher ethylene ion dosage. The observed red and blue shifts were attributed to adsorption of CO stabilized by a proposed direct interaction mechanism involving neighboring surface O atoms and C-containing species, respectively. In the case of low-energy ion irradiation of a N-precovered Cu(100) surface in ethylene, EELS features attributable to C$\equiv$N and N–H stretching vibrations were observed, giving support to the formation of CN and NH radicals as a result of surface reactions between the hydrocarbon species and the pre-deposited N atoms. The present work provides further evidence for in-situ formation and stabilized adsorption of unique surface species generated by the low-energy ion irradiation process.

Keywords: Alkenes; Amorphous surfaces; Chemisorption; Copper; Electron energy loss spectroscopy (EELS); Ion bombardment; Low index single crystal surfaces; Nitrogen; Oxygen; Surface chemical reaction; Thermal desorption spectroscopy

1. Introduction

The chemisorption and surface reactions of hydrocarbons on metal surfaces have continued to be the subjects of intense investigation in surface science. Of particular interest is the dissociative chemisorption of hydrocarbons on transition metal surfaces, such as platinum and related bimetallic alloys, because of their applications in hydrocarbon catalysis [1]. In particular, hydrocarbon adsorbates were reported to undergo sequential C–H bond breaking and skeletal rearrangement between 340 K and 700 K to produce chemically active hydrocarbon fragments, which became an integral part of the catalytic surface [2]. As the simplest unsaturated hydrocarbon with a single π bond, ethylene has often been used as a model system for studying chemisorption on metal surfaces. For instance, decomposition of chemisorbed

* Corresponding author. Fax: (+1) 519 746 0435; e-mail: tong@uwaterloo.ca

0039-6028/98/$19.00
PII: S0039-6028(97)01093-5

ethylene has been found to occur on various transition metal surfaces (including Pt, Pd, Rh, Ru, and Ni) [1] and is believed to lead to the formation of such novel surface species as ethylidyne, vinylidene and vinyl radicals [1,3]. Similar decomposition processes have, however, not been observed for noble metal surfaces. Furthermore, unlike the chemisorption of ethylene on most transition metal surfaces, which involves di-σ or rehybridization bonding to the substrate, ethylene usually retains most of its π bonding character when adsorbed on noble metal surfaces [such as Cu(100) and Ag(110)] [3,4]. In practice, ethylene was found to adsorb molecularly on Cu(100) only at a low temperature ($\sim$80 K) with the π bond parallel to the surface, and to undergo molecular desorption when the temperature was increased. Also found were a number of characteristic vibrations for ethylene adsorbed at 80 K, which include the C–H out-of-plane bending mode at 901 cm^{-1}, the C–H scissoring mode at 1287 cm^{-1}, the C=C stretch at 1553 cm^{-1} and the C–H stretch at 2984 cm^{-1} [5].

In recent years, new technologies involving ion or plasma-assisted surface reactions have been widely used for developing novel materials [6]. In particular, various organic thin films deposited on metal and semiconductor surfaces have been achieved by activating hydrocarbon reactants with low-energy ion beams or plasmas. In these applications, the reactive carbonaceous species were found to play a crucial role in the formation of these thin films [7]. Because the reaction mechanisms of surface reactions involving ion-activated hydrocarbon species are fundamentally different from that of thermal gas-surface reactions, it is of practical interest to investigate the adsorption properties and surface chemistry of hydrocarbon fragments created by ion irradiation. Depending on the impact energy of the ions, other processes (such as ion implantation and creation of defect sites) can also occur concurrently with reaction activation during ion irradiation [8]. The interrelations among the ion-induced effects of different processes are particularly intriguing.

In the present work, we investigate the dissociative chemisorption induced by low-energy ion irradiation in ethylene at room temperature (RT) on clean, O-precovered, and N-precovered Cu(100) surfaces by high-resolution electron energy loss spectroscopy (EELS) and temperature-programmed desorption (TPD) mass spectrometry. Due to the potential complexities of the ion-induced effects, we choose a relatively unreactive and well-defined surface such as Cu(100) for the aforementioned studies. Together with pre-exposures of O and N atoms, we can extend these studies to investigate the interactions between the pre-deposited atoms and ethylene ions and their fragments. Examining the possible initial surface products from these ion-surface reactions is of practical interest to applications in catalysis and thin films deposition. In particular, hydrocarbon fragments produced during ion irradiation in ethylene at RT are found to react with clean, O-precovered, and N-precovered Cu(100) surfaces to form different surface species. In the case of clean Cu(100), the EELS results suggest "stabilized" chemisorption of hydrocarbon species up to $\sim$600 K. On an O-precovered Cu(100) surface, we find evidence for the coexistence of CO with these hydrocarbon species. In particular, both red- and blue-shifted CO stretching modes are observed in the EELS spectra at high ethylene ion dosage [above 1000 L (1 L = 1×10^{-6} Torr-second)]. Since detailed discussions on the production of CO at RT involving a low ethylene ion dose on an O-precovered Cu(100) surface and on the possible mechanisms for the observed red shift in the CO stretching frequency have been given in our earlier work [9], the present work focuses on effects induced by a high dose of ethylene ions. In the case of low-energy ethylene ion interactions with a N-precovered Cu(100) surface, the presence of CN and NH species generated in situ on the surface during ion irradiation is inferred from the observed EELS features attributable to C$\equiv$N and N–H stretching modes. Other effects due to defect sites created by low-energy ion irradiation are also investigated.

2. Experimental method

The experiments were conducted in a triple-level ultra-high vacuum (UHV) chamber (base pres-

sure $<8\times10^{-11}$ Torr), equipped with an ion (sputtering) gun, a four-grid retarding-field optics for low-energy electron diffraction (LEED) and Auger electron spectroscopic (AES) analyses, and a 1–300-a.m.u. quadrupole mass spectrometer (QMS) for TPD studies [10]. The EELS spectra were obtained at 4 eV impact energy in a specular reflection geometry (45° from the surface normal) using a home-built angle-resolved EELS spectrometer described elsewhere [10,11]. Due to the surface roughening effects created by ion irradiation in the experiment, the effective energy resolution was degraded from 64 cm^{-1} full width at half maximum (FWHM) for a typical clean Cu(100) surface to 80–120 cm^{-1} FWHM after ion irradiation. The absolute peak positions could be determined to an accuracy of ±16 cm^{-1} (or 2 meV) due to the broadened peaks. The Cu(100) sample (9.5 mm diameter $\times$ 2 mm thick) at 99.999% purity was obtained commercially from Monocrystals Company. The sample was cleaned by repeated cycles of Ar^+ sputtering [at 500 eV and 10 mA (electron emission current) in an ambient Ar pressure of 2×10^{-5} Torr] and annealing to 850 K, until a sharp (1×1) LEED pattern and no detectable Auger peaks attributable to the common impurities (such as C, O and S) were obtained. The sample could be heated to $\sim$900 K using a boron nitride heater in contact with the backside of the substrate (with a 0.05-mm-thick Ta foil placed between the heater and the Cu sample). The surface temperature of the sample was monitored by a type K thermocouple (mechanically fastened to the front face of the sample) to an absolute accuracy of ±20 K. During the TPD experiments, the front face of the crystal was positioned less than 0.5 mm from an orifice that provided the only entrance to a differentially pumped chamber that housed the QMS. Such an arrangement was found to be effective in lowering the background and preventing desorbed species in the surrounding from entering the ionizer region. The temperature was varied at a linear heating rate of 1 K s^{-1} with a precision better than ±1 K. Ethylene, oxygen (both at 99.99% purity) and nitrogen (at 99.9% purity) were purchased from Matheson, and ethylene-d_4 (at 98% purity) was obtained from Cambridge Isotope Laboratories, Inc. All the gaseous samples were used without further purification. All exposures were carried out by using a variable leak valve, with the pressure monitored by an uncalibrated ionization gauge.

Ion irradiation without mass selection was performed by operating the ion gun in an ethylene ambient pressure of 1×10^{-6} Torr. The ion flux delivered to the sample was estimated to be 10 nA mm^{-2}. The ion dose can be calculated from the product of the ion flux and the exposure time [obtained from the exposure in units of L (Langmuir) and the pressure employed (1×10^{-6} Torr)]. For example, the ion dose obtained from ion irradiation with 1 L of ethylene is $\sim10^{11}$ ions mm^{-2}. The sample was positioned 5 cm from the front face of the ion gun during the ion irradiation experiments. The impact energy (IE) of the ion beam could be controlled by adjusting a floating voltage applied on the sample with respect to a preselected beam energy of the ion gun. In the present experimental setup, ethylene was ionized by electrons with 200 eV kinetic energy inside the ion gun, and only positive ions from the ion gun could reach the sample without mass selection. A cracking pattern of ethylene revealed that the parent ions, $C_2H_4^+$, are the majority ions, with other smaller ions such as $C_2H_3^+$, $C_2H_2^+$, C_2H^+, CH_2^+ and CH^+ present with decreasing concentrations [12]. When the ions collide with the surface, they may become neutralized or may dissociate further into other smaller fragments including carbon and hydrogen atoms. The resulting radicals may in turn undergo reactions with the substrate atoms or pre-deposited atoms (O or N) to form stable surface species at RT.

3. Results and discussion

3.1. Low-energy ethylene ion interactions with clean Cu(100)

In an earlier study by Nyberg, Tengstal and Andersson, C_2H_4 was found to adsorb molecularly on clean Cu(100) only at low temperature [5]. In our previous work [11], the AES results for Cu(100) exposed at RT to a relatively low dose

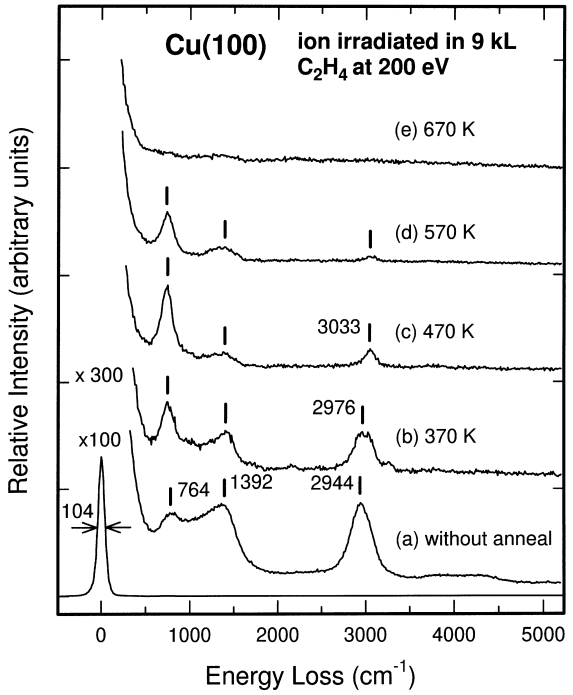

Fig. 1. Electron energy loss spectra for (a) a clean Cu(100) surface ion-irradiated in 9 kL of C_2H_4 at 200 eV impact energy, and for sample (a) annealed to (b) 370 K, (c) 470 K, (d) 570 K and (e) 670 K.

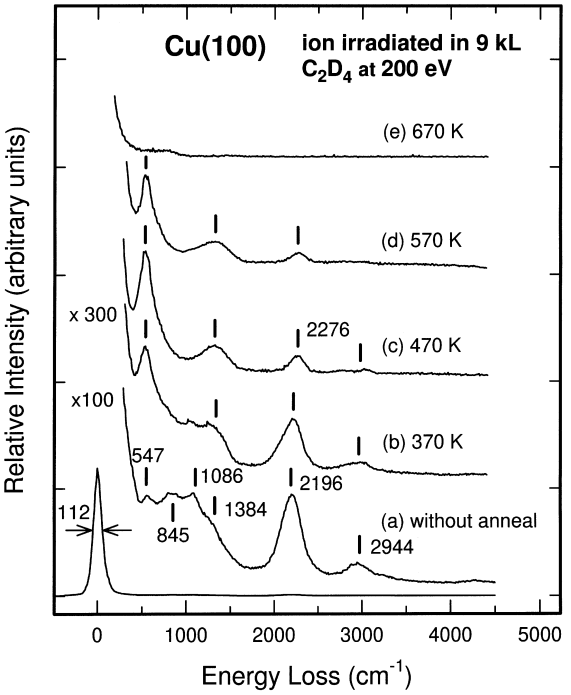

Fig. 2. Electron energy loss spectra for (a) a clean Cu(100) surface ion-irradiated in 9 kL of C_2D_4 at 200 eV impact energy, and for sample (a) annealed to (b) 370 K, (c) 470 K, (d) 570 K and (e) 670 K.

[0.6 kL (1 kL = 1000 L)] of ethylene ions at a low IE of 50 eV indicated the presence of surface carbon on the Cu(100) sample without any discernible EELS feature. However, if the ion dosage and IE were increased, several prominent features were observed in the EELS spectra. Fig. 1 shows the EELS spectra recorded after different annealing temperatures for a clean Cu(100) surface ion-irradiated in 9 kL of C_2H_4 at 200 eV IE. After ion irradiation at RT (Fig. 1a), the sample exhibited a diffused (1×1) LEED pattern, which became sharper with increasing annealing temperature. In the corresponding EELS spectra (Fig. 1a–d), three broad bands centered at 764, 1392 and 2944 cm^{-1} were observed. Each of the bands appeared to be made up of several peaks that could not be resolved by our spectrometer, because the effective resolution was degraded by the roughened surface caused by ion irradiation. In order to identify the observed EELS features, we replaced C_2H_4 with deuterated ethylene (C_2D_4) for ion irradiation and repeated the same experiment. The corresponding EELS spectra shown in Fig. 2 reveal that the bands at 547 and 2196 cm^{-1} can be assigned, respectively, to the isotope-shifted features at 764 and 2944 cm^{-1} for the C_2H_4 case shown in Fig. 1a. The broad structure between 547 and 1086 cm^{-1} in Fig. 2a can be attributed to the isotope-shifted features in the 764–1392 cm^{-1} region in Fig. 1a. The small peak at 2944 cm^{-1} in Fig. 2 is due to the presence of residual C_2H_4 in our 98% pure C_2D_4 sample. However, the broad band centered at 1384 cm^{-1} (which becomes more evident in Fig. 2c and d) is found to be at essentially the same energy loss position as that at 1392 cm^{-1} in Fig. 1. This feature is therefore not related to hydrogen and can be assigned to the stretching mode of a C=C bond. The characteristic stretching frequencies for the single and double C-to-C bonds in common hydrocarbons in the gas phase are generally located at $\sim$900 cm^{-1} and $\sim$1650 cm^{-1}, respectively [13].

Although the observed frequency ($1392\,cm^{-1}$) is lower than that of a typical C=C double bond ($1650\,cm^{-1}$), this frequency may vary from 1200 to $1600\,cm^{-1}$ depending on the chemisorption geometry (e.g. $1200\,cm^{-1}$ for C_2H_4/Ni(111) [14], $1440\,cm^{-1}$ for C_2H_2/Si(100) [15], and $1570\,cm^{-1}$ for C_2H_4/Ni(100) [3]). The broadness of this band may be due to contributions from hydrocarbon species with a C=C bond adsorbed with different adsorption structures. In addition to the C=C contribution, the peak at $1392\,cm^{-1}$ in Fig. 1a may also contain contribution from CH scissors modes, which are located in the same frequency region [16]. It should be noted that changing either the ethylene ion dosage between 4 kL and 32 kL or the IE between 50 eV and 500 eV in general only affects the overall intensities but not the widths of the EELS features. EELS spectra with similar intensities could be obtained if ion irradiation was performed for an amorphous Cu surface [obtained by sputtering Cu(100) in 2×10^{-5} Torr of Ar for 30 min at 500 eV IE]. However, direct dosing of ethylene without ion irradiation on an amorphous Cu surface did not give rise to any kind of adsorption, which indicates that the presence of defect sites did not play an important role in the observed adsorption.

In comparison with molecular adsorption of C_2H_4 on Cu(100) at low temperature [5], there are several notable differences in the observed vibrational features obtained by ion irradiation at RT. The broad feature centered at $2944\,cm^{-1}$ (Fig. 1a) suggests the presence of overlapping C–H stretching modes (symmetric and asymmetric) in several hydrocarbon species, in marked contrast to the C_2H_4/Cu(100) system at 80 K, which exhibited a sharp peak corresponding to a symmetric stretching mode (asymmetric mode was not observed because of the smaller cross-section) [5]. In the low-temperature adsorption case, the sharp peak at $1553\,cm^{-1}$ was assigned to the stretching vibration of a C=C double bond [5]. In the present experiment, no corresponding peak was observed near this energy loss. Instead, the broad feature located at a lower frequency of $1392\,cm^{-1}$ (Fig. 1a) is indicative of adsorbates with a weakened C=C bond involving possibly quite different adsorption arrangements. Although the features between 764 and $1392\,cm^{-1}$ in Fig. 1 (or those between 547 and $1086\,cm^{-1}$ for C_2D_4 in Fig. 2) are not resolved, contributions from other modes (rock, twist, wag and scissors modes) of different hydrocarbon fragments are possible. The most intense feature also occurs at a different location ($764\,cm^{-1}$ in Figs. 1b–d) from the low-temperature adsorption case ($901\,cm^{-1}$), which was assigned to an out-of-plane C–H bending mode [5]. The difference in the frequencies and the observed RT adsorption suggest that the dominant species involve a different adsorption configuration from the π-bonded geometry found for C_2H_4 in the low-temperature adsorption case.

The vibrational frequencies along with their tentative assignments for the EELS features obtained in the present ion-irradiation experiment are compared with those of the corresponding features for C_2H_4/Cu(100) at 80 K [5], gaseous C_2H_4 [13], and the CH_2 functional group [16] in Table 1. Fig. 3 illustrates some of the plausible adsorption structures of ethylene-derived hydrocarbon species on Cu(100). The di-σ bonding configuration of the ethen-1,2-diyl radical ($\overset{|}{H}C\overset{||}{C}H$) shown in Fig. 3a can be regarded as a resonance structure of the single-σ bonding one of the vinyl (ethenyl, $-C_2H_3$) radical with the loss of a hydrogen atom (Fig. 3b). Similarly, the "bridge" configuration of the methylene ($>CH_2$) radical (Fig. 3d) together with the gain or loss of an adsorbed H atom may be considered as a reso-

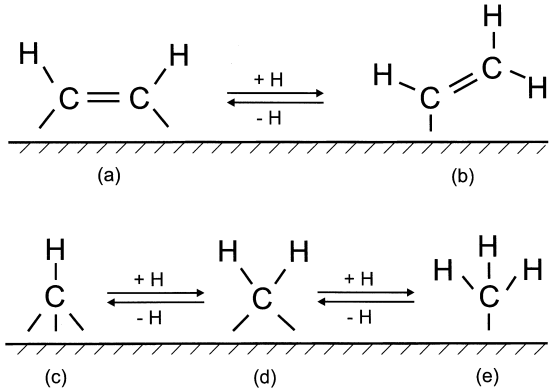

Fig. 3. Plausible hydrocarbon species adsorbed on Cu(100) after low-energy ion irradiation in ethylene at room temperature.

Table 1
Comparison of vibrational frequencies (cm^{-1}) of the observed species on Cu(100) at room temperature obtained by ion irradiation in C_2H_4 at 200 eV (this work) with those obtained by molecular adsorption at 80 K and those for C_2H_4 and CH_2 group in the gas phase

Mode	This work	C_2H_4/Cu(100) at 80 K [5]	C_2H_4 [13]	CH_2 [16]
C–H stretch	2944–3033 (2196–2276)	2984 (2229)[a]	3009 (2245)	2990 (2241)[b] 2932 (2145)[a]
C=C stretch	1392 (1384)	1553 (1416)	1617 (1520)	—
CH_2 scissors	1392 (1086)	1287 (949)	1336 (981)	1447 (1103)
Out-of-plane bend	764 (547)[c]	901 (676)	949 (660)	1267 (996) wag 1213 (877) twist
CH_2 rock		—	—	875 (668)

Values for the deuterated analogs are given in parentheses.
[a]Symmetric stretch; [b]asymmetric stretch; [c]part of a broad feature.

nance structure of the atop configuration of the methyl ($\rightarrow CH_3$) radical (Fig. 3e) or that of the methine (–CH) radical (Fig. 3c) (likely in a four-fold hollow site), respectively. Since the C–H stretching frequencies for the different adsorption configurations are quite close to one another [16], the broadness of the observed EELS features precludes us from unambiguously identifying the nature of the adsorbed hydrocarbon species, observed in the aforementioned and all of the low-energy ethylene ion irradiation experiments (discussed below) in the present work. Indeed, the adsorption of a combination of the aforementioned species (Fig. 3) is likely and could account for the observed broad peaks (e.g. at $2944\ cm^{-1}$). Adsorption of different hydrocarbon fragments at different adsorption sites may also contribute to the observed broad features. It should be noted that other structures including vinylidene (ethen-1,1-diyl, $>CCH_2$) and acetylide (CCH), observed on Pt(111) and related transition metal surfaces [1], are less likely on a (100) fcc surface, though these structures cannot be ruled out from our data [17].

When the sample was annealed to 370 K (Fig. 1b), the band at $764\ cm^{-1}$ became sharper and more evident while the relative intensities of the other two bands were reduced. The center of the band at $2944\ cm^{-1}$ (Fig. 1a) was also shifted to $2976\ cm^{-1}$ (Fig. 1b). Upon further annealing the sample to 470 K (Fig. 1c), the peak at $764\ cm^{-1}$ remained strong while the band at $1392\ cm^{-1}$ became very weak. The band at $2976\ cm^{-1}$ (Fig. 1b) was reduced to a small peak at $3033\ cm^{-1}$ (Fig. 1c). Only the peak at $764\ cm^{-1}$ remained evident after the 570 K anneal (Fig. 1d), and all the peaks were removed after further annealing to 670 K (Fig. 1e). These changes with increasing annealing temperature indicate that the adsorbed hydrocarbon species underwent decomposition at different temperatures. At 470 K (Fig. 1c), only C–H stretching, C=C stretching and C–H out-of-plane bending modes are clearly discernible. Among the five proposed hydrocarbon species shown in Fig. 3, only the ethen-1,2-diyl radical has just these three modes, which suggests that other adsorbed species decomposed at a temperature below 470 K. This assignment is also consistent with the apparent shift in the C–H stretching frequency from $2944\ cm^{-1}$ to $3033\ cm^{-1}$ upon annealing because the C–H stretching frequency in the ethen-1,2-diyl radical is generally higher than that of other species [16].

The decomposition of hydrocarbon species is also supported by the TPD results shown in Fig. 4. Due to the relatively high hydrogen background in our chamber, the TPD experiments were performed on the deuterated sample used in Fig. 2a. Only recombinative desorption of deuterium (corresponding to mass 4) was found over the temperature range 360–660 K. Because no other deuterated hydrocarbon species was detected in the TPD study, deuterated hydrocarbon species must have undergone complete decomposition on the surface in this temperature range. The multiple-

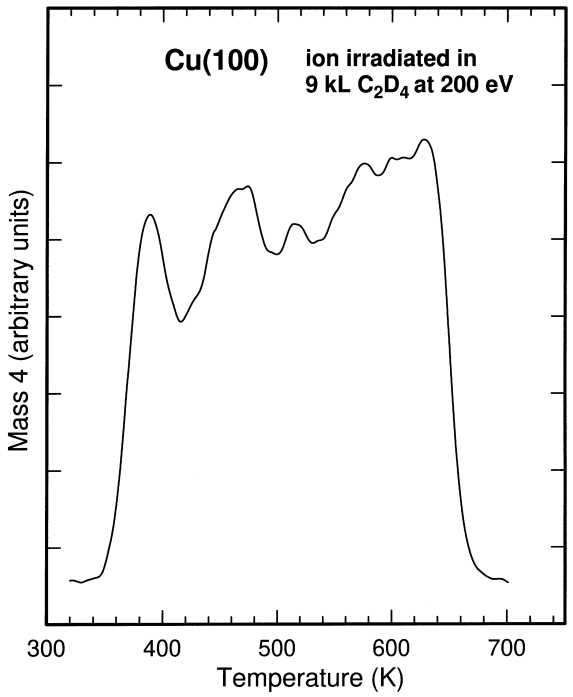

Fig. 4. Temperature-programmed desorption profile of the parent ion (mass 4) of deuterium for Cu(100) ion-irradiated in 9 kL of C_2D_4 at 200 eV impact energy.

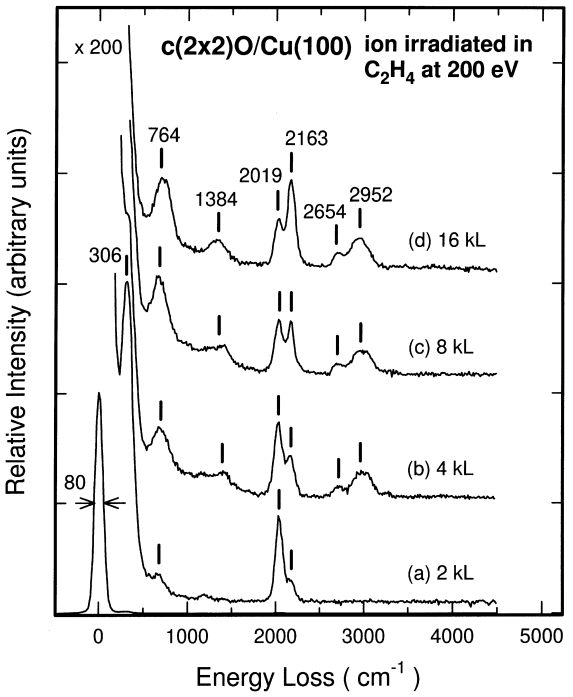

Fig. 5. Electron energy loss spectra for an oxygen-precovered Cu(100) surface ion-irradiated at 200 eV impact energy in (a) 2 kL, (b) 4 kL, (c) 8 kL and (d) 16 kL of C_2H_4.

peak structure of the mass-4 TPD profile in Fig. 4 suggests the presence of many desorption phases (pathways) for D_2, indicating different sources of D atoms as a result of thermal decomposition of the adsorbed hydrocarbon species. The desorption of embedded hydrogen due to ion implantation could also contribute to the observed desorption profile. TPD results have also been obtained for different ion dosage and at different impact energies (not shown). In these cases, the overall intensities of the desorption profiles were found to be different while the temperature range over which desorption occurred remained unchanged.

3.2. Low-energy ethylene ion interactions with O-precovered Cu(100)

An oxygen-covered Cu(100) surface can be obtained by directly exposing O_2 to Cu(100) at RT ([18] and references therein). Our previous studies showed that ion irradiation of an O-precovered Cu(100) surface in ethylene below 600 L at RT resulted in RT adsorption of CO stabilized by coadsorbed O atoms [9,11]. At a higher dose of ethylene ions, however, the adsorption of both CO and hydrocarbon species (Fig. 3) is evident. Fig. 5 shows the EELS spectra for a $c(2\times2)O/Cu(100)$ sample as a function of ethylene ion dosage. At an ethylene ion dose of 2 kL (Fig. 5a), the dominant features are the Cu–O stretch at 306 cm^{-1} and the red-shifted C–O stretch at 2019 cm^{-1}. (It should be noted that in spite of the multiple bond order in CO, we have followed the earlier convention when writing C–O stretch [5,9,11], in which CO should not be interpreted as "single-bonded".) The observed red shift in the C–O stretch has been previously proposed to be caused by direct interaction between a pre-deposited O atom and an as-formed CO molecule [produced in situ by the reaction: C (ad.)+O (ad.)→CO (ad.)] [11]. At a higher ethylene ion dose, the EELS spectra (Fig. 5b–d) reveal the hydrocarbon features at 764, 1384 and 2952 cm^{-1}, which are consistent with their assign-

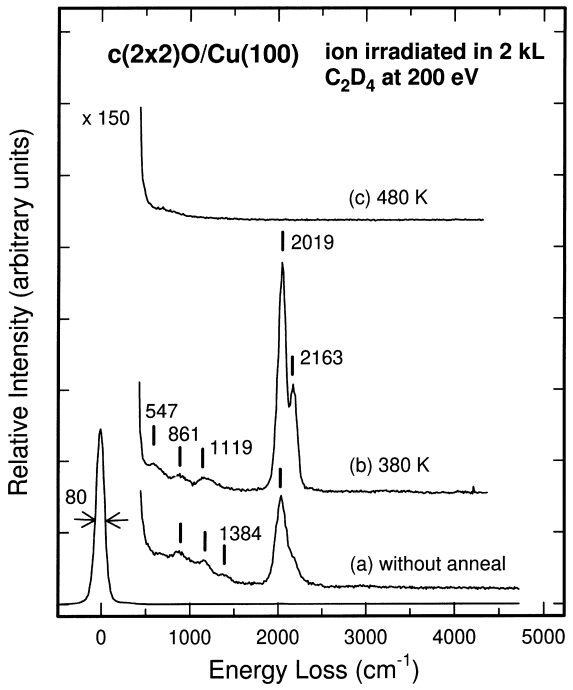

Fig. 6. Electron energy loss spectra for an oxygen-precovered Cu(100) surface ion-irradiated at 200 eV impact energy in 2 kL of C_2D_4 (a) without and with annealing to (b) 380 K and (c) 480 K.

ments to C–H out-of-plane bend, C=C stretch and C–H stretch, respectively, as depicted in Fig. 1. In addition to the red-shifted C–O stretch at 2019 cm^{-1}, the peak at 2163 cm^{-1}, which first appeared only as a small shoulder at a low ion dose (Fig. 5a), became stronger with increasing ion dosage. In order to identify the nature of this peak, we conducted an isotope substitution experiment with a 2 kL ion dose of C_2D_4. In addition to the previously observed features attributed to deuterated hydrocarbon species found in the corresponding Cu(100) case (Fig. 2) and the red-shifted CO stretch at 2019 cm^{-1}, the corresponding EELS spectra shown in Fig. 6 indicate the presence of a shoulder at 2163 cm^{-1} (Fig. 6a). The identical position of this peak to that found in the spectrum for the normal ethylene case (Fig. 5a) confirms that this peak is not related to vibrations involving H. The feature at 2163 cm^{-1} became more evident after annealing to 380 K (Fig. 6b). The data obtained with a higher dose of deuterated ethylene ions are not presented here because the peak at 2163 cm^{-1} would be masked by a much stronger peak corresponding to the C–D stretch, which happened to occur at almost the same frequency (Fig. 2). As in our previous work, we propose that the feature at 2163 cm^{-1} corresponds to a "perturbed" C–O stretch, with its frequency blue-shifted from its nominal position at 2089 cm^{-1} (found in the low-temperature adsorption case) [19]. This blue-shifted feature could be the result of direct interaction between an as-formed CO and a nearby C or hydrocarbon species (Fig. 3) produced in the ion irradiation process. In this model, a neighboring C or hydrocarbon species may deplete electrons in the $2\pi^*$ anti-bonding orbital of the CO molecule, hence strengthening the C≡O triple bond and causing a blue shift in the C–O stretching frequency. The direct interaction between CO and a C or hydrocarbon neighbour gives rise to a C–CO or hydrocarbon–CO quasi-complex that stabilizes CO on Cu(100) at RT. The observed double-peak structure can therefore be attributed to the formation of these quasi-complexes, i.e. O–CO for the red-shifted CO peak and C–CO or hydrocarbon–CO for the blue-shifted CO peak, at different locations of the surface. This model is also consistent with the fact that the relative intensity of the peak at 2163 cm^{-1} to that of the peak at 2019 cm^{-1} increased with increasing dosage of ethylene ions, which should increase the hydrocarbon concentration at the expense of the O coverage on the surface (Fig. 5). Although the surface-mediated (indirect) interactions of O and C with CO could also give rise to blue and red shifts in the C–O stretching frequency, respectively, as previously suggested for CO on Mo(110) [20], such indirect interaction would not produce the stabilizing effect observed in our experiment. A further increase in the ethylene ion dosage to 32 kL (not shown) caused a reduction in the intensities of the CO peaks, while the peaks corresponding to the hydrocarbon fragments became stronger, which indicates that oxygen and CO were removed from the surface due to sputtering effects in the ion irradiation process.

Fig. 7 shows the EELS spectra for a c(2×2)O/Cu(100) sample ion-irradiated with

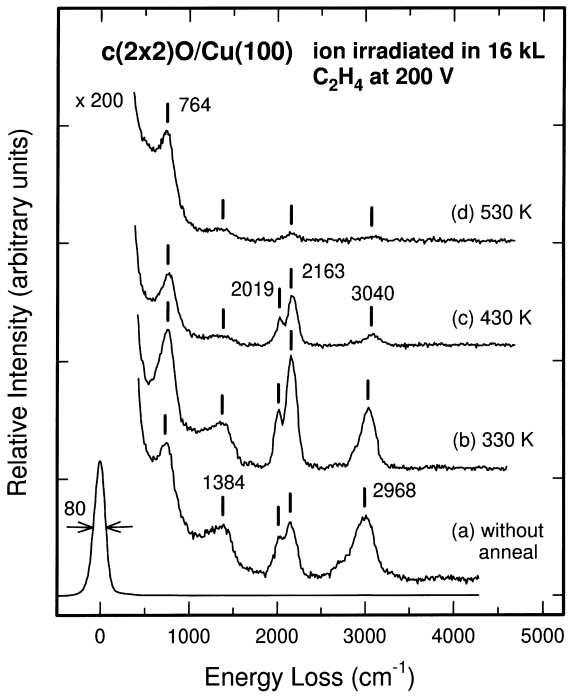

Fig. 7. Electron energy loss spectra for an oxygen-precovered Cu(100) surface ion-irradiated at 200 eV impact energy in 16 kL of C_2H_4 (a) without and with annealing to (b) 330 K, (c) 430 K and (d) 530 K.

16 kL of ethylene at RT (Fig. 5d) as a function of annealing temperature. The corresponding coadsorbed hydrocarbon species apparently exhibit energy loss features at 764, 1384 and 2968 cm^{-1} (Fig. 7a), similar to those found for the Cu(100) case shown in Fig. 1a. These hydrocarbon features also vary in a similar fashion with increasing annealing temperature as that depicted in Fig. 1. Furthermore, the stabilized CO peaks at 2019 cm^{-1} and 2163 cm^{-1} became more intense when the sample was annealed to 330 K (Fig. 7b) but weakened upon further annealing to a higher temperature (Fig. 7c and d). The observed temperature dependence is therefore similar to that of the oxygen-stabilized CO peak observed in our earlier work [11]. The corresponding TPD result (not shown) for the sample prepared at a lower dose (8 kL) of deuterated ethylene ions indicates desorption of deuterium (D_2) from the surface between 370 K and 650 K (again similar to the results shown in Fig. 4), and that CO desorption occurred at $\sim$420 K (similar to the behaviour reported by us earlier) [11]. No other ions (of different masses) were found during the TPD process, which further supports the postulate of complete decomposition of hydrocarbon species on the surface. These results indicate that different initial surface conditions of a c(2×2)O overlayer did not significantly affect the adsorption structure of the hydrocarbon species deposited subsequently using the ion irradiation technique. Since no direct evidence for the formation of any surface species containing the C=O or C–O functional group was obtained, it appears that surface oxygen only reacted with atomic carbon produced during ion irradiation to form C≡O.

3.3. Low-energy ethylene ion interactions with N-precovered Cu(100)

Although N_2 does not readily adsorb on Cu(100) at RT, a c(2×2)N overlayer can be obtained by low-energy electron or ion irradiation in N_2 at RT followed by annealing to 550 K [8]. The nitrogen atoms were reported to adsorb in the fourfold hollow sites [21]. Fig. 8 shows the EELS spectra of a c(2×2)N/Cu(100) sample after ion irradiation in 5 kL of ethylene followed by annealing to different temperatures. Evidently, the broad band at 2944 cm^{-1} corresponding to the C–H stretch observed in Fig. 1a is replaced by a prominent and much sharper peak at 3379 cm^{-1} in Fig. 8a, which cannot be assigned to contributions related to hydrocarbon species due to its significantly higher frequency. Also shown in Fig. 8a are two weak, broad features at 2091 cm^{-1} and 2735 cm^{-1}. Furthermore, the broad features below 1500 cm^{-1} cannot be clearly resolved. The corresponding EELS spectra for an isotope substitution experiment are shown in Fig. 9. The peak at 3379 cm^{-1} in Fig. 8a has an isotope-shifted analog at 2445 cm^{-1} in Fig. 9a, while the peak at 2091 cm^{-1} in Fig. 8a remains at essentially the same position in the deuterated ethylene case (Fig. 9a). The vibrational frequencies of the features obtained for the ion irradiation case and their tentative assignments are compared with the corresponding features for gaseous HCN [22],

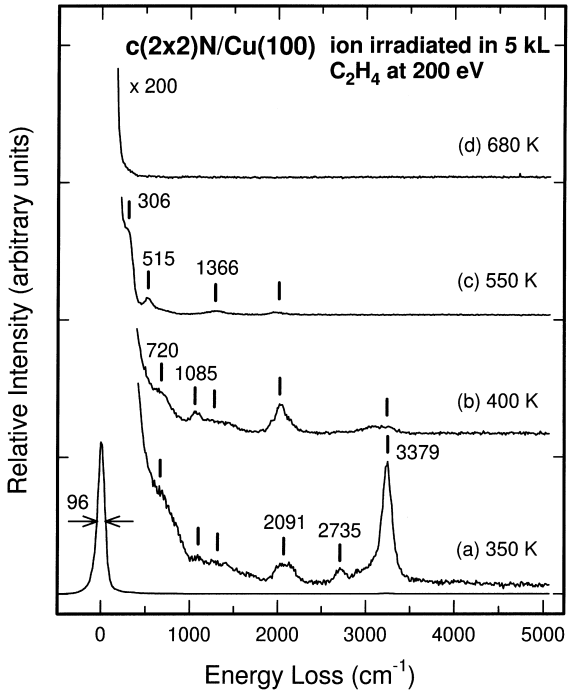

Fig. 8. Electron energy loss spectra for a nitrogen-precovered Cu(100) surface ion-irradiated at 200 eV impact energy in 5 kL of C_2H_4 and annealed to (a) 350 K, (b) 400 K, (c) 550 K and (d) 680 K.

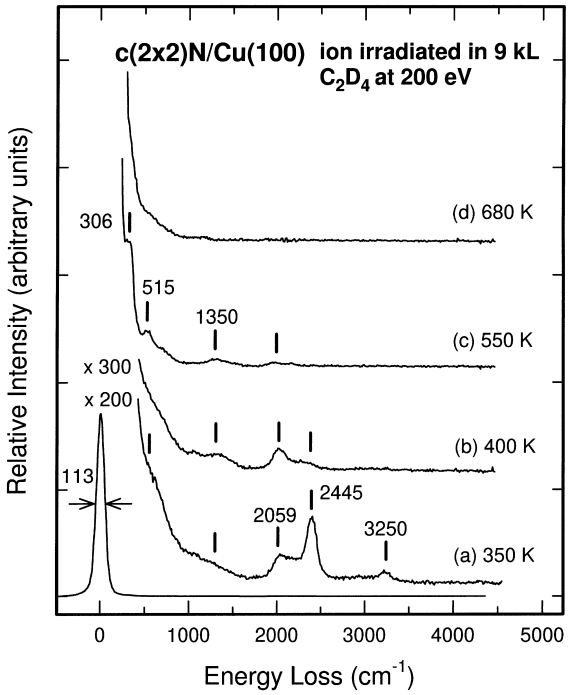

Fig. 9. Electron energy loss spectra for a nitrogen-precovered Cu(100) surface ion-irradiated at 200 eV impact energy in 9 kL of C_2D_4 and annealed to (a) 350 K, (b) 400 K, (c) 550 K and (d) 680 K.

gaseous HNC [22], HCN/Cu(111) [23], and HCNH/W(100) [24,25] in Table 2.

In accordance with the earlier studies [23,26], the peak at 2091 cm^{-1} (Fig. 8) can clearly be assigned to a C≡N stretching mode in a cyanide related adsorbate. The peak at 2735 cm^{-1} in Fig. 8a could be assigned to a "perturbed" C–H stretch in the hydrocarbon fragments produced by ion irradiation (Fig. 3). The assignment for the peak at 3379 cm^{-1} (Fig. 8) is, however, less clear, and there are three possibilities. The first possibility is C–H stretch in a hydrogen cyanide (HCN) adsorbate. In keeping with the representative vibrational frequencies reported for the common hydrocarbon groups [16], a C–H stretching frequency as high as 3330 cm^{-1} can only be found in the methylidyne (≡C–H) radical. Because it is unlikely that carbon forms a triple bond to a single Cu atom directly, the bonding to Cu must involve a N atom through the formation of H–C≡N (hydrogen cyanide). In this model, the energy loss feature observed at 2091 cm^{-1} can be assigned as a C≡N stretch [23]. However, although the C–H stretching frequency for HCN has been found to be 3312 cm^{-1} in a matrix-isolation experiment and 3441 cm^{-1} in the gas phase [22], it usually occurs at a lower frequency for a HCN adsorbate on a metal surface. For example, the C–H stretch was reported at 3145 cm^{-1} for condensed HCN [27], 3121 cm^{-1} for HCN/Cu(111) [23], and 2940 cm^{-1} for HCNH/W(100) [24,25]. The presently observed frequency at 3379 cm^{-1} may therefore be too high to be assigned as a C–H stretch in an adsorbed HCN molecule. The second possible assignment for this peak is the N–H stretching mode in a hydrogen isocyanide (HNC) adsorbate. Although the N–H stretching frequency for matrix-isolated HNC is 3653 cm^{-1} and that for gaseous HNC is 3842 cm^{-1} [22,26], it has also been observed at 3360 cm^{-1} for a HCNH intermediate on a W(100) surface [24,25]. These frequencies are quite similar to that observed in the present

Table 2
Comparison of vibrational frequencies (cm^{-1}) of the observed species obtained on N-precovered Cu(100) by ion irradiation in C_2H_4 at 200 eV (this work) with those for gaseous HCN, gaseous HNC, HCN/Cu(111), and HCNH/W(100)

Mode	This work	HCN [22]	HNC [22]	HCN/Cu(111) [23]	HCNH/W(100) [24,25]
N–H stretch	3379	—	3842 (3653)	—	3360
C–H stretch	2735	3441 (3312)	—	3121	2940
C≡N stretch	2091	2127 (2097)	2067 (2029)	2068	—
C=N stretch	—	—	—	—	1400
C=C stretch	1366	—	—	—	—
XCN bend	515[a]	727 (714)[b]	490 (477)[b]	821[b]	—
Cu–N stretch	306	—	—	—	—

Values for the corresponding matrix isolated samples of HCN and HNC are given in parentheses.
[a]X = C or N; [b]X = H.

work ($3379\ cm^{-1}$). The third possibility is that the NH_x ($x = 1$–3) and cyanide (C≡N) radicals coexist separately on the surface, which could also give rise to the peaks at $3379\ cm^{-1}$ for N–H stretch and $2091\ cm^{-1}$ for C≡N stretch. Among the possible NH_x species (NH, NH_2 and NH_3), the most likely adsorbate is the NH radical because of the high activation barriers in the hydrogenation reaction pathways from NH to NH_2 and to NH_3 [28]. Furthermore, although the N–H stretching frequencies for the three possible NH_x species could locate between $3300\ cm^{-1}$ and $3400\ cm^{-1}$ [29], the presence of NH_2 or NH_3 is expected to produce a broader N–H feature due to additional asymmetric stretching modes. It is therefore unlikely that the observed single peak at $3379\ cm^{-1}$ (Fig. 8a) would contain contributions from the NH_2 or NH_3 species. In this model, the peak at $3379\ cm^{-1}$ could be assigned to a N–H stretch with NH in a fourfold hollow site, while the peak at $2091\ cm^{-1}$ could be assigned to a C≡N stretch with CN in an upright position [30]. Among the three possible assignments for the $3379\ cm^{-1}$ peak, we favour the last model involving the coexistence of CN and NH radicals on the surface because additional energy is required for the formation of HCN or HNC in the other models.

The peak at $3379\ cm^{-1}$ can apparently be removed at a lower annealing temperature (400 K, Fig. 8b) than the peak at $2091\ cm^{-1}$, which indicates that breaking the N–H bond requires less energy than breaking the Cu–CN bond. As discussed below, the desorption of NH radical was not observed in the TPD experiments, indicating the thermal dissociation of NH. After the sample was annealed to 550 K, the peak at $515\ cm^{-1}$ became more evident in both samples prepared with normal ethylene ions (Fig. 8c) and deuterated ethylene ions (Fig. 9c). This feature could be attributed to a XCN bending mode, where X is a neighboring C or N atom [31]. This proposed bonding picture is similar to the direct interaction model, involving as-formed CO stabilized by neighboring O or C-containing species, discussed above. The weak broad feature at $1366\ cm^{-1}$, which can clearly be seen in Fig. 8c (and Fig. 9c), could be assigned to a C=C stretch as discussed above. The shoulder at $306\ cm^{-1}$ found in both Figs. 8c and 9c is due to Cu–N stretch [21]. Finally, all the energy loss features were removed after the samples were annealed to 680 K (Figs. 8d and 9d).

Fig. 10 shows the corresponding TPD profiles for the deuterated sample used in Fig. 9. Desorption profiles for mass 4 (corresponding to D_2), mass 28 and 14 (corresponding to N_2), and mass 26 (corresponding to CN) were recorded. Mass 4 came from recombinative desorption of deuterium atoms originated from thermally dissociated N–D radicals and embedded deuterium atoms. The maximum CN desorption observed in the TPD experiment occurred at ~680 K, which is inconsistent with the temperature range (350–550 K) over which the peak reduction of the C≡N stretch occurred (Figs. 9a–c). This indicates

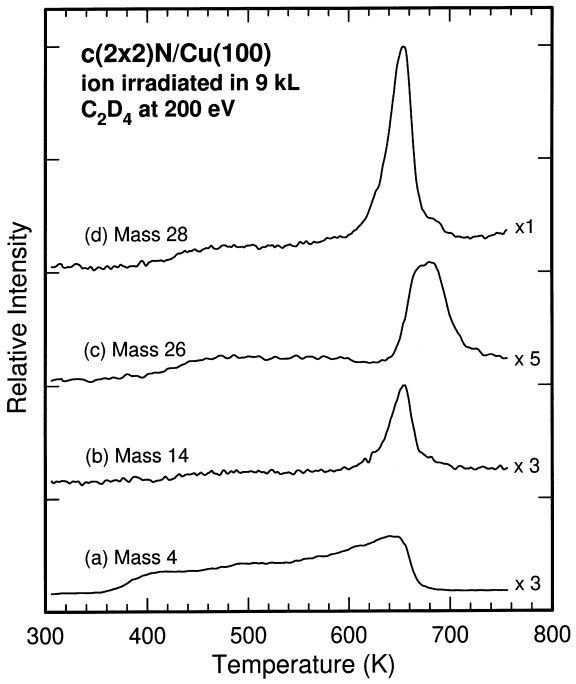

Fig. 10. Temperature-programmed desorption profiles of the parent ions of (a) D_2 (mass 4), (c) CN (mass 26) and (d) N_2 (mass 28), and of (b) mass 14 (corresponding to the N atoms dissociated from N_2 in the ionizer) for a nitrogen-precovered Cu(100) surface ion-irradiated in 9 kL of C_2D_4 at 200 eV impact energy.

that the CN species desorbed at 680 K in the TPD experiments came from recombinative desorption of surface C and N atoms. The disappearance of the CN features in the EELS spectra below 550 K can be explained by the decomposition of the as-formed CN radical. Desorption of mass 28 came from recombinative desorption of the N atoms in the $c(2\times2)$N/Cu(100) substrate [8]. It should also be noted that no HCN or HNC (mass 27) nor DCN or DNC (mass 28) species could be found in the TPD experiments for the samples used in Figs. 8 and 9, respectively, which supports the model of separate adsorption of CN and NH (ND) radicals instead of that of HCN (DCN) or HNC (DNC) on the surface. The relative intensity of hydrogen to nitrogen desorption is found to increase with increasing ethylene ion dosage or impact energy, which indicates that the nitrogen species could be displaced from the surface by ethylene ion irradiation.

4. Concluding remarks

In the present work, we have studied the adsorption induced by low-energy ion irradiation in ethylene without mass selection at RT on clean, O-precovered and N-precovered surfaces of Cu(100) by high-resolution EELS and TPD mass spectrometry. We demonstrated the effectiveness of low-energy ion irradiation in generating stabilized surface species, which cannot be obtained otherwise by normal gas–surface thermal reactions. By using standard surface analysis techniques such as EELS and TPD, we found the coexistence of several adsorbates under different surface conditions at RT. In particular, the adsorption of different hydrocarbon species (Fig. 3) on a clean Cu(100) surface could be produced in situ by low-energy ion irradiation in ethylene. These hydrocarbon species underwent decomposition upon annealing, and their characteristic EELS features could be observed at a temperature as high as $\sim$600 K. In the case of an O-precovered surface, we observed the presence of both red-shifted and blue-shifted C–O stretching modes, which are attributed to as-formed CO stabilized by direct interactions with, respectively, nearby O and C-containing species generated by irradiation with a heavy dose of low-energy ethylene ions. In the case of a N-precovered surface, surface nitrogen atoms were found to react with the hydrocarbon fragments generated by ion irradiation to produce CN and NH (containing) species on the surface. The reactions of ethylene ions with a N-precovered Cu(100) surface therefore appear to be quite different from those with an O-precovered surface. The formation of NH (containing) species indicates that the hydrocarbon fragments must undergo some forms of dissociation to produce H on the N-covered surface in order for the subsequent reaction(s) with surface nitrogen to occur. In all cases studied in the present work, low-energy ion irradiation played a crucial role in both the formation and stabilized adsorption of these surface species.

Acknowledgements

This work was supported by the Natural Sciences and Engineering Research Council of Canada.

References

[1] G.A. Somorjai, Introduction to Surface Chemistry and Catalysis, Wiley-Interscience, New York, 1994.
[2] D.A. King, D.P. Woodruff (Eds.), The Chemical Physics of Solid Surfaces and Heterogeneous Catalysis, Vol. 4, Chapter 7, Elsevier, Amsterdam, 1982, p. 217.
[3] F. Zaera, R.B. Hall, Surf. Sci. 180 (1987) 1.
[4] N. Sheppard, J. Electron Spectrosc. Relat. Phenom. 38 (1986) 187.
[5] C. Nyberg, C.G. Tengstal, S. Andersson, Chem. Phys. Lett. 87 (1982) 87.
[6] D.L. Smith, Thin Film Deposition Principles and Practice, Chapter 8, McGraw-Hill, New York, 1995.
[7] C.C. Cheng, P.A. Taylor, R.M. Wallace, H. Gutleben, L. Clemen, M.L. Colaianni, P.J. Chen, W.H. Weinberg, W.J. Choyke, J.Y. Yates, Jr., Thin Solid Films 225 (1993) 196.
[8] H. Yu, K.T. Leung, J. Vac. Sci. Tech. A 16 (1998) 30.
[9] H. Yu, K.T. Leung, Surf. Sci. 335 (1996) L355.
[10] D.Q. Hu, PhD thesis, University of Waterloo, Waterloo, 1993.
[11] H. Yu, D.Q. Hu, K.T. Leung, J. Vac. Sci. Technol. A 15 (1997) 2653.
[12] Eight Peak Index of Mass Spectra, Vol. 1, Mass Spectrometry Data Center, Aldermaston, 1974.
[13] G. Herzberg, Molecular Spectra and Molecular Structure: Infrared and Raman Spectra of Polyatomic Molecules, Vol. 2, Van Nostrand, Toronto, 1945.
[14] S. Lehwald, H. Ibach, Surf. Sci. 89 (1979) 499.
[15] W. Widdra, C. Huang, S.I. Yi, W.H. Weinberg, J. Chem. Phys. 105 (1996) 5605.
[16] H. Ibach, D.L. Mills, Electron Energy Loss Spectroscopy and Surface Vibrations, Academic Press, New York, 1982.
[17] L.L. Kesmodel, G.D. Waddill, J.A. Gates, Surf. Sci. 138 (1984) 464.
[18] M. Wuttig, R. Franchy, H. Ibach, J. Electron Spectrosc. Relat. Phenom. 44 (1987) 317.
[19] S. Andersson, Surf. Sci. 89 (1979) 477.
[20] W.K. Kuhn, J.W. He, D.W. Goodman, in: D.J. Dwyer, F.M. Hoffmann (Eds.), Surface Science of Catalysis, ACS Symposium Series 482, 1992, p. 71.
[21] M.H. Mohamed, L.L. Kesmodel, Surf. Sci. 185 (1987) L467.
[22] T.J. Lee, C.E. Dateo, B. Gazdy, J.M. Bowman, J. Phys. Chem. 97 (1993) 8937.
[23] M.E. Kordesch, W. Feng, W. Stenzel, M. Weaver, H. Conrad, J. Electron Spectrosc. Relat. Phenom. 44 (1987) 149.
[24] J.G. Serafin, C.M. Friend, J. Phys. Chem. 92 (1988) 6694.
[25] C.M. Friend, J.G. Serafin, J. Chem. Phys. 88 (1988) 4037.
[26] D.E. Milligan, M.E. Jacox, J. Chem. Phys. 39 (1963) 712.
[27] H.B. Friedrich, P.F. Krause, J. Chem. Phys. 59 (1977) 4942.
[28] N. Takehiro, K. Mukai, K. Tanaka, J. Chem. Phys. 103 (1995) 1650.
[29] I.C. Bassignana, K. Wagemann, J. Kuppers, G. Ertl, Surf. Sci. 175 (1986) 22.
[30] K. Hermann, W. Moller, P.S. Bagus, J. Electron Spectrosc. Relat. Phenom. 39 (1986) 107.
[31] A.J. Capote, A.V. Hamza, N.D.S. Canning, R.J. Madix, Surf. Sci. 175 (1986) 445.